horticulturae

MDPI

Article

miR398 Attenuates Heat-Induced Leaf Cell Death via Its Target CSD1 in Chinese Cabbage

Biting Cao [1,2,†], Jianxia Jiang [3,†], Jinjuan Bai [2], Xuan Wang [2], Yajie Li [2], Wenna Shao [4], Shengwu Hu [1,*], Yuke He [2,*] and Xiang Yu [4,*]

1 State Key Laboratory of Crop Stress Biology in Arid Areas and College of Agronomy, Northwest A&F University, Xianyang 712100, China; caobis@163.com
2 National Key Laboratory of Plant Molecular Genetics, Center for Excellence in Molecular Plant Science, Shanghai Institute of Plant Physiology and Ecology, Chinese Academy of Sciences, Fenglin Road 300, Shanghai 200032, China; jjbai@cemps.ac.cn (J.B.); doublexzz@outlook.com (X.W.); yjli02@sjtu.edu.cn (Y.L.)
3 Crop Breeding and Cultivation Research Institute, Shanghai Academy of Agricultural Sciences, Shanghai 201403, China; xiajianjiang321@163.com
4 Joint International Research Laboratory of Metabolic & Developmental Sciences, School of Life Sciences and Biotechnaology, Shanghai Jiao Tong University, Shanghai 200240, China; swn_9511@sjtu.edu.cn
* Correspondence: swhu83251@nwafu.edu.cn (S.H.); heyk@sippe.ac.cn (Y.H.); yuxiang2021@sjtu.edu.cn (X.Y.); Tel.: +86-29-8708-2604 (S.H.); +86-21-5492-4111 (Y.H.); Fax: +86-21-5492-4111 (Y.H.)
† These authors contribute equally to this work.

Abstract: Previous research has shown that miR398 contributed to plant thermotolerance by silencing its target gene *COPPER/ZINC SUPEROXIDE DISMUTASE1* (*CSD1*) in *Arabidopsis thaliana*. However, the phylogenesis of miR398 and *CSD1* in Brassica crop and their role in regulating leaf cell death under heat stress remains unexplored. Here, we characterized the homologous genes of miR398a and *CSD1* in *Brassica rapa* ssp. *pekinensis* (Chinese cabbage) and found miR398a abundance was accumulated under heat stress (38 °C and 46 °C for 1 h) in Chinese cabbage, while the expression level of its targets *BraCSD1-1* and *BraCSD2-1* were downregulated. To further explore their role in heat response, we constructed the transgenic plants overexpressing artificial miR398a (aBra-miR398a), Bra-miR398a target mimic (Bra-MIM398a), and *BraCSD1-1* in Chinese cabbage for genetic study. Under high temperatures, *p35S::aBra-miR398a* lines reduced the areas of leaf cell death and delayed the leaf cell death. By contrast, *p35S::Bra-MIM398a* and *p35S::BraCSD1-1* plants enlarged the areas of leaf cell death and displayed the earliness of leaf cell death. Finally, we found that the expression level of stress-responsive genes *BraLEA76*, *BraCaM1*, *BraPLC*, *BraDREB2A*, and *BraP5CS* increased in transgenic plants overexpressing aBra-miR398a, which may contribute to their resistance to heat-induced leaf cell death. Taken together, these results revealed the function of Bra-miR398a in attenuating leaf cell death to ensure plant thermotolerance, indicating that the miR398-CSD1 module could be potential candidates for heat-resistant crop breeding.

Keywords: *Brassica rapa*; cell death; *CSD1*; heat resistance; miR398

Citation: Cao, B.; Jiang, J.; Bai, J.; Wang, X.; Li, Y.; Shao, W.; Hu, S.; He, Y.; Yu, X. miR398 Attenuates Heat-Induced Leaf Cell Death via Its Target CSD1 in Chinese Cabbage. *Horticulturae* **2022**, *8*, 299. https://doi.org/10.3390/horticulturae8040299

Academic Editor: Young-Doo Park

Received: 10 March 2022
Accepted: 26 March 2022
Published: 31 March 2022

1. Introduction

As an integral part of the plant lifecycle, the death of cells, organs, and eventually the whole plant is an age-dependent process. Programmed cell death (PCD) is an essential process determining plant growth and development. It is divided into two broad categories: developmentally regulated and environmentally induced and it plays a key role in the self-destruction of cells damaged by stress factors [1–4]. The leaf is the primary photosynthetic organ for energy harvesting and nutrient production at the growth and maturation stages [5]. The visible yellowing and whitening are widely used to stage the progression of senescence and leaf cell death [6,7]. Leaf senescence occurs at the final stage of leaf development and precedes cell death. At the senescence stage, nutrients accumulated in the leaves were relocated to other organs, such as developing seeds [5,7].

Plant microRNAs are a group of endogenous, 20–24 nucleotides, small non-coding RNAs, and play crucial roles in post-transcriptional regulation by binding its targeted mRNAs for cleavage or repressing translation [8–10]. miR398 is a conserved miRNA that was identified in *Arabidopsis thaliana* by sequence analysis of stress-treated *Arabidopsis thaliana* small-RNA libraries [11,12], which is encoded by three gene loci: MIR398a, MIR398b and MIR398c, and miR398 has been mainly characterized based on the role of its target genes *CSD1* (*SOD1* or *Cu/Zn SUPEROXIDE DISMUTASE1*), *CSD2* (*SOD2*) and *CCS* (*copper chaperone of CSDs*) [13,14]. miR398 play key roles in developmental processes and multiple stress responses [9,11,12,15]. *CSD1* and *CSD2* are the genes regulating the synthesis of cytosolic Cu/Zn-SOD and chloroplast Cu/Zn-SOD, respectively [16]. The two Cu/Zn superoxide dismutase enzymes are responsible for the dismutation of the toxic superoxide to molecular oxygen and hydrogen peroxide in the cytosol by CSD1 or chloroplast by CSD2 together with CCS, which are generally involved in abiotic stress responses [17]. As a negative regulator of CSDs, miR398 is inhibited by oxidative stress during high light, high concentration of heavy metal, or herbicide, resulting in the increase in their targeted mRNAs *CSD1* and *CSD2* [18]. Under other stress, such as ozone fumigation, salt, *Pseudomonas syringae* infection, the abundance of miR398 was also downregulated, implying an important post-transcriptional regulation role of miR398 in these stress responses [9,17–21].

High temperature, one of the most detrimental stresses in nature, is known to affect almost all aspects of plants during growth, causing severe retardation in development and a dramatic decrease in yield [22–24]. The ability to survive after direct extreme heat challenge is termed basal thermotolerance, which is the foundation of all approaches carried by plants to withstand or to acclimate to damage caused by heat [22]. Followed by exposure to sub-lethal high temperatures, plants obtained the power to survive at lethal heat conditions, referred to as acquired thermotolerance [22,25,26]. *B. rapa* is one of the most important leaf vegetable crops, and Chinese cabbage is highly sensitive to heat stress [27]. On the other hand, the premature leaf cell death of Chinese cabbage usually causes the losses of leaf yield and quality [27]. We have found that enhancing miR398 processing results in stronger plant thermotolerance in *Arabidopsis thaliana* [13]. In this study, we characterized the miR398 and its target *CSD1* in *B. rapa* and explored their function in plant thermotolerance-associated leaf cell death. For this purpose, we studied the effects of expression levels of miR398 and its targeted genes on leaf cell death in *Brassica rapa* ssp. *pekinensis*.

2. Materials and Methods

2.1. Plant Materials and Growth Condition

The seeds of *B. rapa* ssp. *pekinensis* (Bre) were used in our experiments [28]. All the seeds including the Bre as wild-type and the transgenic plants were surface-sterilized and sown on Petri dishes containing Murashige and Skoog (MS) medium [28]. After the Petri dishes were sealed with Parafilm, they were stratified at 4 °C in the dark for at least three days and then moved to a growth room and incubated under 16/8 h of light/darkness per day at 22 °C. Ten days later, the seedlings were transplanted to soil (PINDSTRUP, Denmark, Germany) in plastic pots and moved from a growth room to a greenhouse in the phytotron at the Shanghai Institute of Plant Physiology and Ecology (16 h light/8 h dark). Plants were watered at intervals of three to four days [28,29]. For detecting heat-responsive gene expression, the plants were grown at 38 °C for 3 h and 6 h, respectively, or grown at 38 °C and 46 °C for 1 h, respectively. For heat-induced leaf cell death measurement, plants were treated with 45 °C for 12 h followed by 35 °C for 12 h. For the copper treatment experiment, it is worth noting that MS contains trace amounts of copper, 0 μM represents no additional copper added.

2.2. Cloning and Generation of Transgenic Plants

p35S::BraCSD1-1 construct was obtained by PCR using KOD-plus polymerase (ToYoBo, Shanghai, China) with oligonucleotide pairs (BraCSD1-1S and BraCSD1-459A) as defined in the Supplementary Table S1 and the cDNA of *B. rapa* as a template. PCR product was

added to deoxyadenylic acid by rTaq (Takara, Beijing, China), and linked to PMD18T vector, and then were digested with *KpnI* and *XbaI* and cloned in the *KpnI* and *XbaI* sites of pCAMBIA2301.

For construct of *p35S::aBra-miR398a*, the artificial microRNA designer WMD delivers 4 oligonucleotide sequences (I to IV), which were used to engineer artificial microRNA into the endogenous *MIR319a* precursor by site-directed mutagenesis (Supplementary Figure S1). Plasmid pRS300 was used as a template for the PCRs, which contains the *MIR319a* precursor in pBSK [13,30]. The amiRNA containing precursor is generated by overlapping PCR. The first round of amplification fragments was obtained by PCR using KOD-plus polymerase (ToYoBo, Shanghai, China) with the oligonucleotide pairs (amiRNA-A/aBra-miR398-IVa, aBra-miR398-IIa/aBra-miR398-IIIs, and aBra-miR398-Is/amiRNA-B), respectively, as defined in the Supplementary Table S1, and the pRS300 as a template. The second round of amplification was obtained using KOD-plus polymerase (ToYoBo, Shanghai, China) with the oligonucleotide pairs (amiRNA-A/amiRNA-B) as primers and three products from the first round as a template. The products were digested with *KpnI* and *XbaI* and directly cloned in the *KpnI* and *XbaI* sites of pCAMBIA2301 [30,31].

For construct of *p35S::Bra-MIM398a*, the first round of amplification were obtained by PCR using KOD-plus polymerase (ToYoBo, Shanghai, China) with the oligonucleotide pairs (IPS-1S-BamH1/Bra-MIM398a-Ia, Bra-MIM398a-IIs/IPS-522A-Sal1), respectively, as defined in the Supplementary Table S1, and the IPS as template [32]. The second round amplifies were obtained by overlapping PCR using KOD-plus polymerase (ToYoBo, Shanghai, China) with the oligonucleotide pairs (IPS-1S-BamH1/IPS-522A-Sal1) and products (first round) as a template. The products were digested with *BamHI* and *SalI* and directly cloned in the *BamHI* and *SalI* sites of pCAMBIA1301 [13,32]. Three constructs (*p35S::BraCSD1-1*, *p35S::aBra-miR398a*, *p35S::Bra-MIMR398a*) were transformed to *E-coli* DH5α competent cells, and then were delivered into *Agrobacterium tumefaciens* strain GV3101 (pMP90RK) using the freeze-thaw method [33]. The recombinant plasmid was then inserted into *B. rapa* wild-type plants (Bre) via the vernalization–infiltration method as previously described [34].

2.3. Heat Treatment and Measurement of Leaf Cell Death

The leaf with 25% of yellow color was designated as the onset of leaf senescence, while the leaf with flaccid or dried over more than half was designated as the onset of leaf cell death. The day for the onset of leaf senescence was regarded as the first day of leaf senescence while the day for the onset of leaf cell death was regarded as the first day of leaf cell death. The day for whitening of 100% leaf area was termed as the day of leaf death while the day for whitening and browning of all leaves on the plant was regarded as the day of plant death [6]. For heat stress of whole plants, two-week-old seedlings were moved into the soil to grow to the five-leaf stage. Then, these plants were subjected to a heat stress treatment of 45 °C for 12 h followed by 35 °C for 12 h, and then cultivated at 22 °C under long-day conditions (16 h light/8 h dark). Finally, these plants were photographed and analyzed on the 0th, 4th, and 8th days after the heat stress using ImageJ [27].

2.4. miRNA Isolation and Northern Blot Analysis

Total RNA was extracted from 10-day-old seedlings of all plants. Antisense sequences of miR398 were synthesized and end-labeled as probes with biotin (TaKaRa, Beijing, China). The RNA concentration was measured by Nanodrop spectrophotometer, and 15 μg of RNA was fractionated on a 15% polyacrylamide gel containing 8 M urea and transferred to a Nitran Plus membrane (Schleicher and Schuell). Hybridization was performed at 41 °C using hybridization buffer (ULTRAhyb Ultrasensitive Hybridization buffer, Ambion). Autoradiography of the membrane was performed using the LightShift Chemiluminescent EMSA Kit (Pierce). A synthesized U6 probe end-labeled with biotin (TaKaRa, Beijing, China) was used for the quantity control of total RNA content between samples [13,35].

2.5. 5′ RACE (Rapid Amplification of cDNA Ends)

RNA was obtained from 2-week-old seedlings, and 5′ RACE was performed using the RLM-RACE Kit (Invitrogen, Carlsbad, CA, USA) according to its instructions with modification [28]. The 5′ RACE PCR products were excised from the gel and cloned into a pMD18T vector (Takara, Beijing, China) for sequencing. Gene-specific primers for 5′ RACE PCR can be found in Supplementary Table S1.

2.6. Real-Time qRT-PCR

Plant tissues were homogenized in liquid nitrogen and total RNA was extracted from the wild-type and transgenic plants using TRIzol (Invitrogen, Carlsbad, California, USA) and treated with DNaseI (TaKaRa, Beijing China) to remove DNA contamination. Approximately 5 μg of RNA was used for reverse transcription with oligo (dT) primers or stem-loop primers for real-time reverse transcriptase-polymerase chain reaction (qRT-PCR) [36,37]. Real-time qRT-PCR was performed with the Bio-Rad iCycler Thermal CycleriQ5 Multicolor Real-Time PCR machine (Bio-Rad) using iQ SYBR Green Real-Time PCR Supermix (Bio-Rad) according to the manufacturer's instructions [13,29]. The expression of 7 genes (*ACTIN1, ATCIN2, ACTIN3, ACTIN4, ACTIN8, ACTIN11, ACTIN12*) were used as an internal control using degenerate primers [29], and comparative threshold cycle method was used to determine relative transcript levels in real-time qRT-PCR [38]. Real-time PCR for detecting and quantifying miRNAs was performed based on the published protocol [38]. Three biological replicates and three technical replicates were performed for each sample. All the primers used in this study were listed in Supplementary Table S1.

2.7. Sequence Alignment and Phylogenetic Analysis

Arabidopsis thaliana and *B. rapa* pre-miR398 sequences were downloaded from the miRBase (https://www.mirbase.org/search.shtml, accessed on 1 March 2022). *Arabidopsis thaliana* AtCSD1, AtCSD2 and AtCCS protein sequences were downloaded from the Arabidopsis Information Resource (https://www.arabidopsis.org/, accessed on 1 March 2022). The homologous proteins in Chinese cabbage were identified based on HMM search from Brassicaceae Database (BRAD, http://brassicadb.cn, accessed on 1 March 2022). Multiple alignments of these protein sequences from *Arabidopsis thaliana* and *Brassica rapa* were performed using ClustalW and GeneDoc [39]. Unrooted phylogenetic trees were constructed from the aligned protein sequences using the neighbor-joining method in MEGA 6.0 with minor modifications [40], and bootstrapping was carried out with 1000 iterations.

2.8. Degradome Analysis

The degradome data (SRR2149955) from flower bud of *B. rapa* ssp. *pekinensis* [41] was downloaded from NCBI. The degradome was analyzed as previously described [42]. Briefly, the adaptor was removed from raw reads using the tool cutadapt with default parameter settings [43]. The trimmed reads were mapped to *BraCSD1-1* cDNA sequence using STAR mapper with default parameter [44]. The 5′ monophosphate (5′P) end reads were extracted and plotted around the miR398 cleavage site at *BraCSD1-1* using a customized R script.

2.9. Statistical Analysis

Statistical significance was calculated by two-tailed Student's *t*-test and error bars indicate SE. p value < 0.05 were considered to be statistically significant.

3. Results

3.1. Characterization of the miR398 and Its Targets Genes in B. rapa

In *Arabidopsis thaliana*, *MIR398* gene family consists of *MIR398a*, *MIR398b*, and *MIR398c*, while their mature miRNA target genes are *AtCSD1*, *AtCSD2*, and *AtCCS* [13,14]. Through alignment of *Arabidopsis thaliana* miR398 and its target genes with *B. rapa* genomic sequences, we found four *Bra-MIR398* genes and six Bra-miR398-targeted homologous genes in *B. rapa* ssp. *pekinensis*. Based on their DNA sequence similarity, *Bra-MIR398a* homologs were

named as *Bra-MIR398a-1* and *Bra-MIR398a-2*, and *Bra-MIR398b* homologs were regarded as *Bra-MIR398b-1* and *Bra-MIR398b-2* (Figure 1A, Table 1 and Supplementary Table S2). It is worth noting that, the 21-nt mature miRNAs produced from *MIR398a* and *MIR398b* contained 1 nt (T/G) difference at the 3′ end in both *Arabidopsis thaliana* and *B. rapa* (Figure 1A). Based on the phylogenic analysis, the miR398-targeted homologous proteins in heading Chinese cabbage were regarded as BraCSD1-1 (Bra031642), BraCSD1-2 (Bra018596), BraCSD2-1 (Bra034394), BraCSD2-2 (Bra011971), BraCCS-1 (Bra016768), and BraCCS-2 (Bra026968), respectively, (Figure 1B, Table 1, and Supplementary Table S1). Next, to explore the tissue distribution of mature miR398a, we collected root, stem, cauline leaves, and inflorescence from the *B. rapa* accession Bre to determine Bra-miR398a abundance in different tissues using northern blotting. The result indicated that Bra-miR398a was accumulated in all these tissues and was most abundant in cauline leaves (Figure 1C).

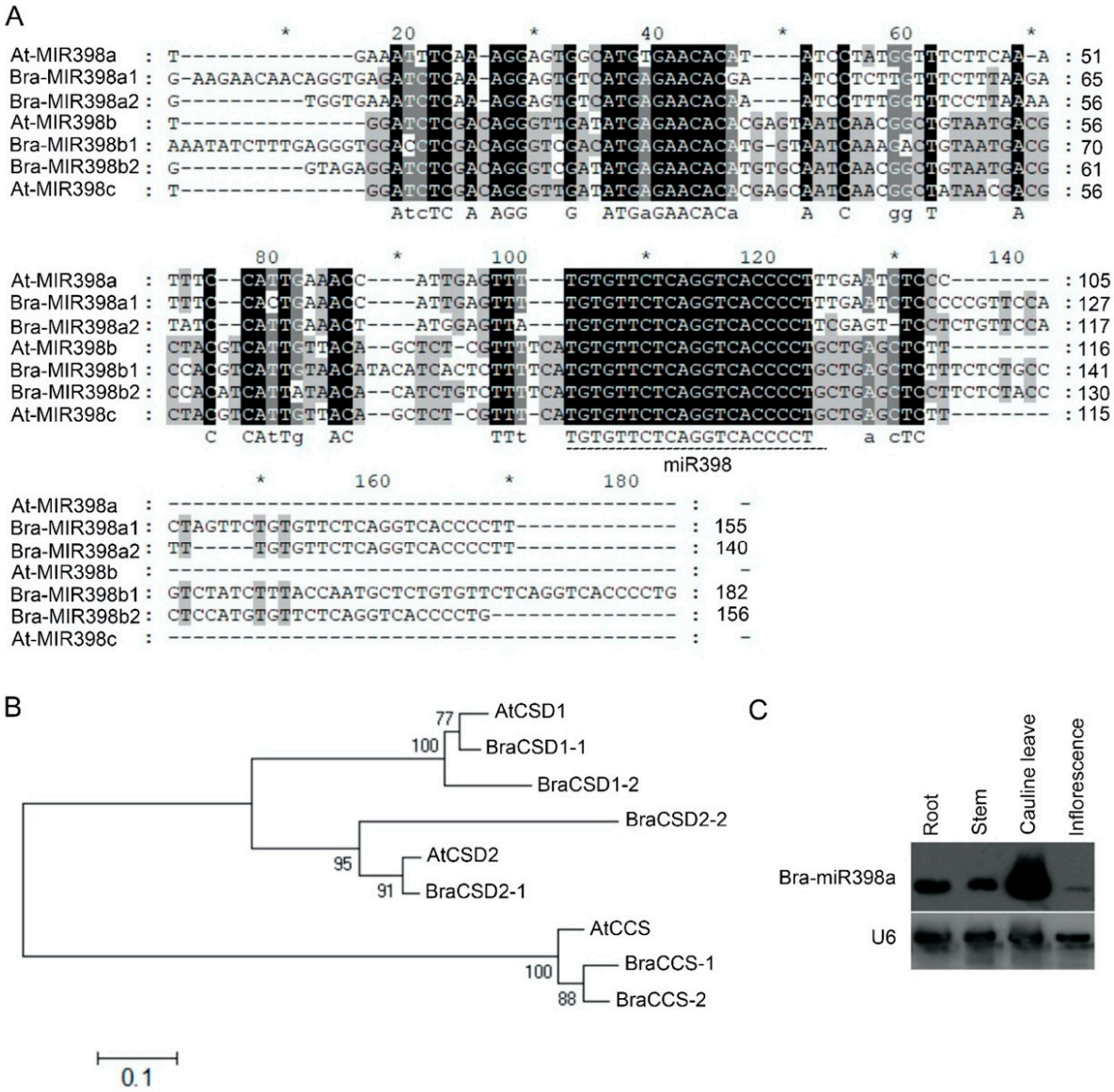

Figure 1. Characterization of miR398 and its targets in *B. rapa*. (**A**) Multiple alignment of pre-miR398 DNA sequences in *Arabidopsis thaliana* and *B. rapa*. The mature miR398 are represented by black solid lines. Asterisks represent 10 bp from the previous number. (**B**) Unrooted phylogenetic trees of miR398 targets based on their protein sequences in *Arabidopsis thaliana* and *B. rapa*. (**C**) Northern blotting showing mature miR398 abundance in different tissues of Bre plants.

Table 1. miR398 and its target genes in *B. rapa*.

miR398 and Targets in *Arabidopsis thaliana*	**Homologous Genes in *B. rapa***
ath-miR398a ath-miR398b ath-miR398c	*Bra-MIR398a1/a2* *Bra-MIR398b1/b2*
AtCSD1 (At1g08830)	BraCSD1-1 (Bra031642) BraCSD1-2 (Bra018596)
AtCSD2 (At2g28190)	BraCSD2-1 (Bra034394) BraCSD2-2 (Bra011971)
AtCCS (At1g12520)	BraCCS-1 (Bra016768) BraCCS-2 (Bra026968)

3.2. Response of Bra-miR398a and Its Target Genes to Heat Stress in B. rapa

In *Arabidopsis thaliana*, mature miR398 is increased under high temperature [45], while in *B. rapa* ssp. *chinensis* (non-heading Chinese cabbage), both mature miR398a and miR398b were declined under heat shock [46]. To investigate the response of Bra-miR398a to heat stress in *B. rapa* ssp. *pekinensis* (heading Chinese cabbage), we used northern blot to detect its accumulation after being treated at 38 °C for 3 h and 6 h, respectively. We found that Bra-miR398a was induced at 38 °C for 3 h, but the accumulation decreased after treatment at 38 °C for 6 h (Figure 2A). Consistent with *Arabidopsis thaliana*, the miR398 target site at *BraCSD1-1* is located at 5′UTR with three mismatches. To confirm the miRNA cleavage at *BraCSD1-1*, 5′ RACE PCR followed by sequencing was used to detect 5′ monophosphate (5′P) end of mRNA degradation intermediates, and the 5′P end of RNAs were frequently detected at positions 10 to 11 of the target region complementary to miR398 (Figure 2B). Consistently, high-throughput degradome profiling from *B. rapa* ssp. *pekinensis* [41] also showed enrichment of 5′P end reads at miR398 cleavage stie of *BraCSD1-1* (Supplementary Figure S2). Using real-time qRT-PCR, we validated that the mature Bra-miR398a were accumulated after treatment at both 38 °C and 46 °C for 1 h (Figure 2C), while the expression of Bra-miR398-targeted *BraCSD1-1* and *BraCSD2-1* were downregulated (Figure 2C). Taken together, we found that Bra-miR398a were accumulated under heat stress in heading Chinese cabbage.

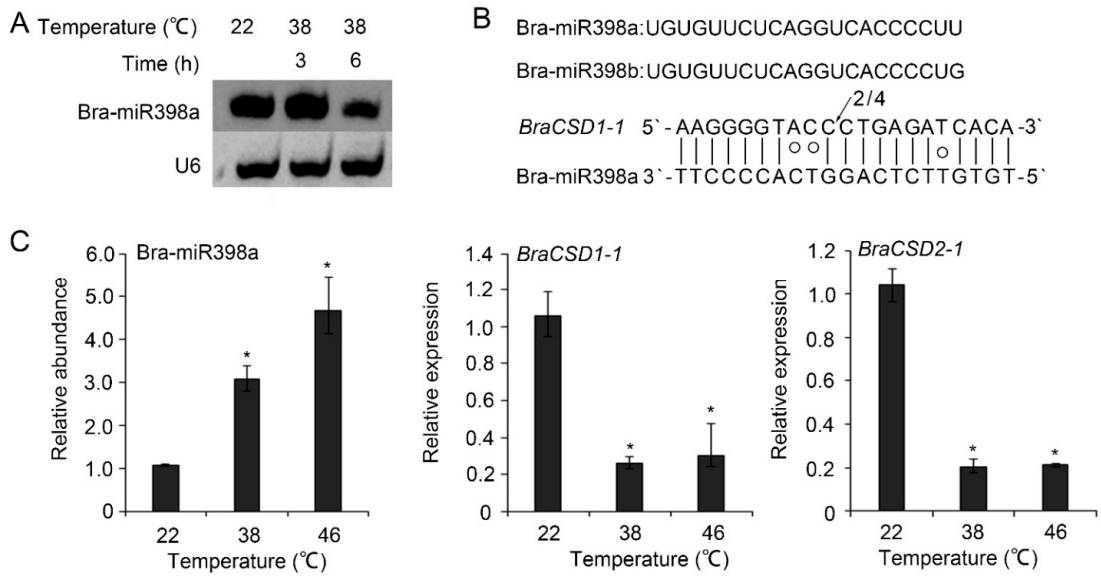

Figure 2. The response of miR398 and its target genes to heat stress. (**A**) Northern blotting showing miR398 abundance under high temperature (38 °C for 3 h and 6 h). (**B**) 5′ RACE PCR showing the cleavage sites of *BraCSD1-1*. Numbers indicate the fraction of cloned PCR products terminating at the position. (**C**) Real-time PCR showing relative abundance of Bra-miR398a and its target genes under 22 °C, 38 °C, and 46 °C for 1 h. The asterisks indicate a significant difference (* represents $p < 0.05$) (Student's *t*-test).

3.3. Bra-miR398a Aids in the Prevention of Leaf Death and Plant Death

As an integral part of plant development, senescence is directly influenced by various exogenous (environmental) factors such as high/low temperatures, drought, ozone, biotic stress, and endogenous (internal) cues including different phytohormones and reproductive development as well as development age of the leaf and plant [47]. The visible yellowing and whitening are widely used to stage the progression of senescence and leaf cell death [6,7]. However, the factors involved in aging are poorly understood. To test whether miR398 was involved in leaf cell death, we constructed transgenic plants in the background of Bre, overexpressing Bra-miR398a (*p35S::aBra-miR398a*) using the backbone of *MIR319a* gene (Supplementary Figure S2), overexpressing Bra-miR398a target mimic (*p35S::Bra-MIM398a*) by modifying the miR398 complementary sequences in *IPS1* [32] (Supplementary Figure S2) and overexpressing one of the miR398 target gene *BraCSD1-1* (*p35S::BraCSD1-1*), using the vernalization–infiltration method [34]. As shown in Figure 3A, the miR398 abundance was increased in *p35S::aBra-miR398a* lines (1#, 2#) while the expression levels of *BraCSD1-1* were up-regulated in *p35S::Bra-MIM398a* (3#, 5#) and *p35S::BraCSD1-1* plants (2#, 5#) (Figure 3A).

To accurately score and characterize the timing and extent of leaf senescence and leaf cell death in whole plants, we measured yellowing and whitening areas of the fourth leaf, counted the number of leaves with cell death in the order of occurrence, and defined leaf cell death and plant survival rates. To demonstrate the processes of leaf cell death, we treated the Bre, *p35S::aBra-miR398a* (1#, 2#), *p35S::Bra-MIM398a* (3#, 5#), and *p35S::BraCSD1-1* (2#, 5#) plants with 45 °C 12 h followed by 35 °C 12 h, and then the plants were moved into a greenhouse at 22 °C under long-day conditions (16-h light/8-h dark) for further growth, along with photographing and analysis on the 0th, 4th, and 8th days, respectively. The growth of the *p35S::Bra-MIM398a* (3#, 5#) and *p35S::BraCSD1-1* (2#, 5#) were significantly weaker than that of the Bre on the fourth day after the high-temperature treatment, while the growth of the *p35S::aBra-miR398a* (1#, 2#) were markedly stronger than that of the Bre (Figure 3B,D). The leaf senescence and leaf cell death of *p35S::Bra-MIM398a* (3#, 5#) and *p35S::BraCSD1-1* (2#, 5#) plants appeared much earlier than the wild-type while the degree of leaf cell death was much higher (Figures 3D and 4). As expected, the yellowing and

whitening area of leaves of the *p35S::aBra-miR398a* (1#, 2#) were smaller than that of the Bre (Figures 3B and 4).

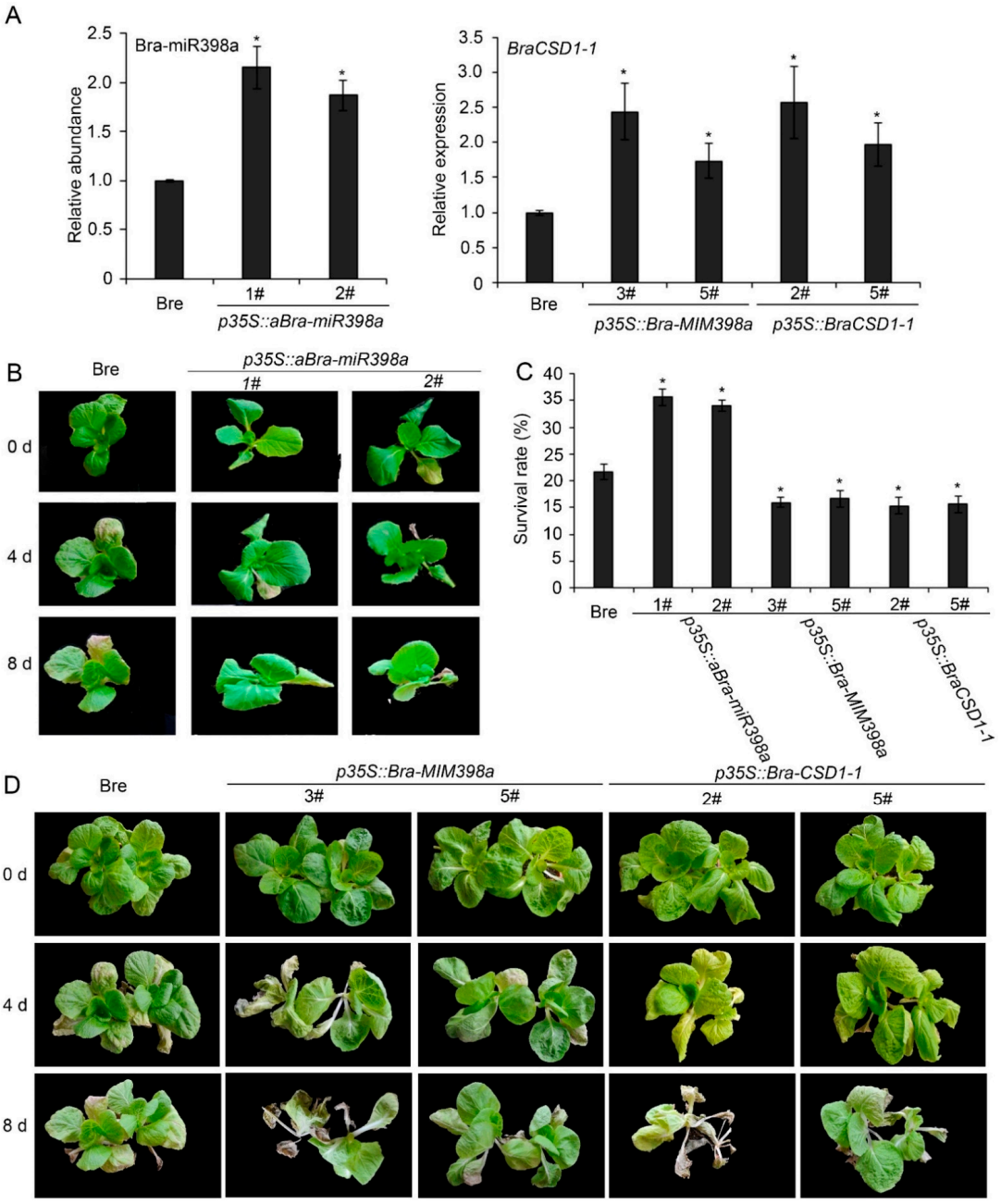

Figure 3. The expression levels of miR398 and *BraCSD1-1* and survival rates of the transgenic plants under heat stress. (**A**) Real-time PCR showing relative abundance of miR398 and relative expression *BraCSD1-1* in the transgenic plants. The asterisks indicate a significant difference (* represents $p < 0.05$) (Student's *t*-test). (**B**) Bre and *p35S::aBra-miR398a* (1#, 2#) plants were photographed and recorded on the fourth and eighth day after high-temperature treatment (45 °C 12 h followed by 35 °C 12 h). (**C**) Survival rates of Bre, *p35S::aBra-miR398a* (1#, 2#), *p35S::Bra-MIM398a* (3#, 5#), and *p35S::BraCSD1-1* (2#, 5#) plants. The asterisks indicate a significant difference (* represents $p < 0.05$) (Student's *t*-test). (**D**) Bre, *p35S::Bra-MIM398a* (3#, 5#), and *p35S::BraCSD1-1* (2#, 5#) plants were photographed and recorded on the fourth and eighth day after high-temperature treatment (45 °C 12 h followed by 35 °C 12 h).

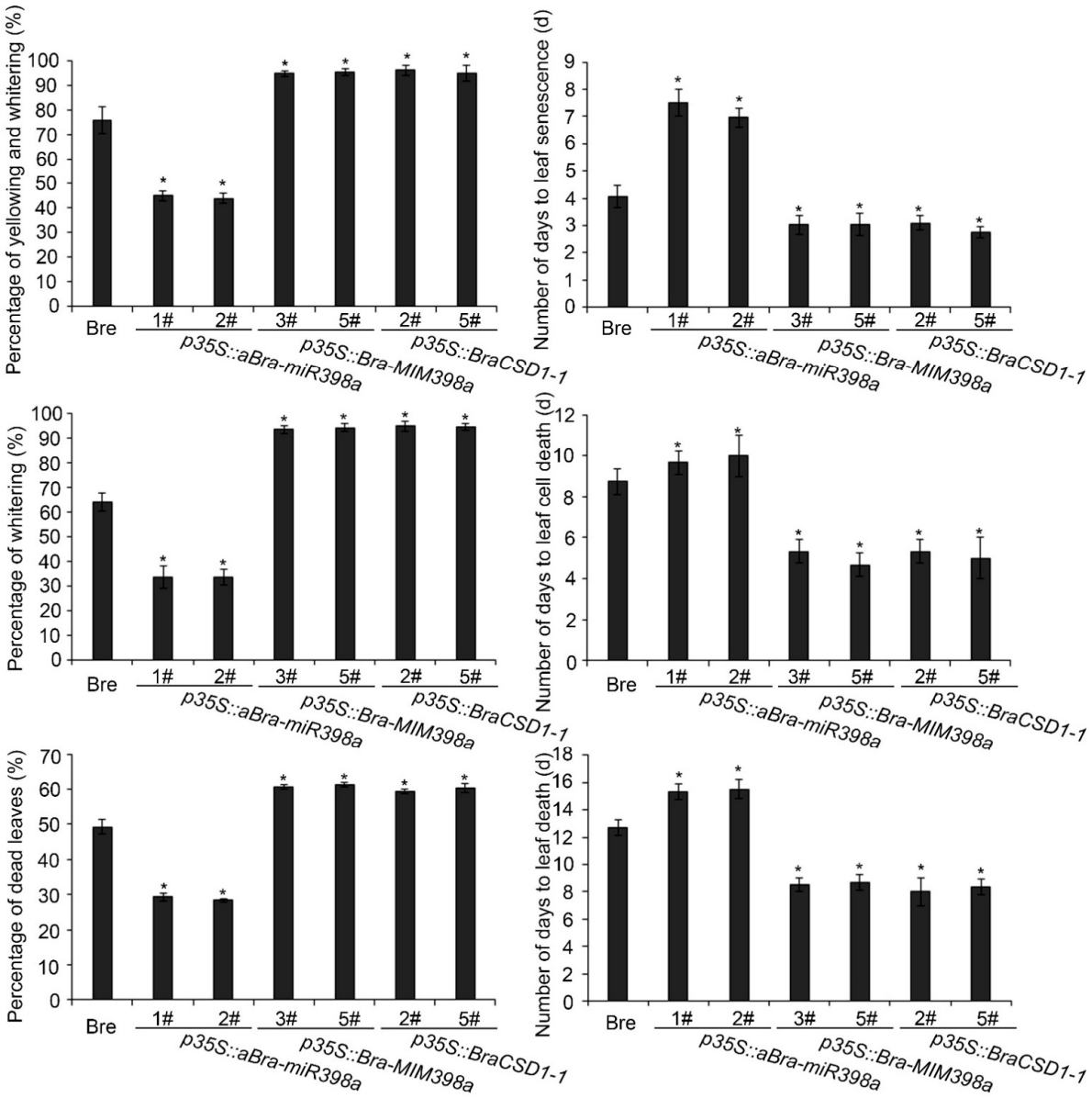

Figure 4. Leaf cell death under high-temperature treatment (45 °C 12 h followed by 35 °C 12 h). The result showed that the percentage of yellow (senescence) and white (cell death) leaf areas, percentage of white leaf areas, percentage of the dead leaves, number of days to senescence, number of days to leaf cell death, and number of days to leaf death of Bre, *p35S::aBra-miR398a* (1#, 2#), *p35S::Bra-MIM398a* (3#, 5#), and *p35S::BraCSD1-1* (2#, 5#) plants. More than 20 leaves for each treatment were harvested and measured from the fourth node of plants. The asterisks indicate a significant difference (* represents $p < 0.05$) (Student's *t*-test).

Leaf cell death is usually followed by leaf death and plant death. Under high-temperature stress, Bre leaves died after 14 days (Figure 4), and survival rates of Bre plants were over 20% (Figure 3C). The leaves of the *p35S::Bra-MIM398a* (3#, 5#) and *p35S::BraCSD1-1* (2#, 5#) plants died on the 10th day after being subjected to high-temperature stress (Figure 4), and the survival rate of the plants was ~15% (Figure 3C). However, the leaves of *p35S::aBra-miR398a* (1#, 2#) plants died on the 16th day after the high-temperature stress treatment (Figure 4), and the survival rate of the plants was 35% (Figure 3C). Compared to the wild-type, the *p35S::aBra-miR398a* (1#, 2#) plants showed a later leaf death, fewer dead leaves, and higher survival rate, but the *p35S::Bra-MIM398a* (3#, 5#) and *p35S::BraCSD1-1* (2#, 5#) plants were completely opposite. These results indicated that heat stress acceler-

ated leaf senescence and leaf cell death, but the accumulation of *MIR398a* can alleviate this process.

3.4. Bra-miR398a Regulated Heat-Induced Leaf Cell Death Independent with Cu^{2+}-Mediated Pathway

miR398 is strictly regulated by Cu^{2+} levels [21]. We surveyed the germination and growth of *p35S::aBra-miR398a* (1#, 2#), *p35S::Bra-MIM398a* (3#, 5#), and *p35S::BraCSD1-1* (2#, 5#) plants on solid MS with 75 μM and 150 μM Cu^{2+} concentrations, respectively. The seedlings of the wild-type and all the transgenic lines were injured heavily under Cu^{2+} stress with 150 μM. However, the leaf color of *p35S::aBra-miR398a*, *p35S::Bra-MIM398a*, and *p35S::BraCSD1-1* transgenic plants were not different from that of the wild-type under Cu^{2+} stress (Figure 5). The *p35S::aBra-miR398a* transgenic plants were more resistant to high temperature, but showed similar sensitivity to the high level of Cu^{2+} as compared to wild-type, suggesting that Bra-miR398a potentially affected the heat-induced leaf cell death independent with Cu^{2+}-mediated pathway.

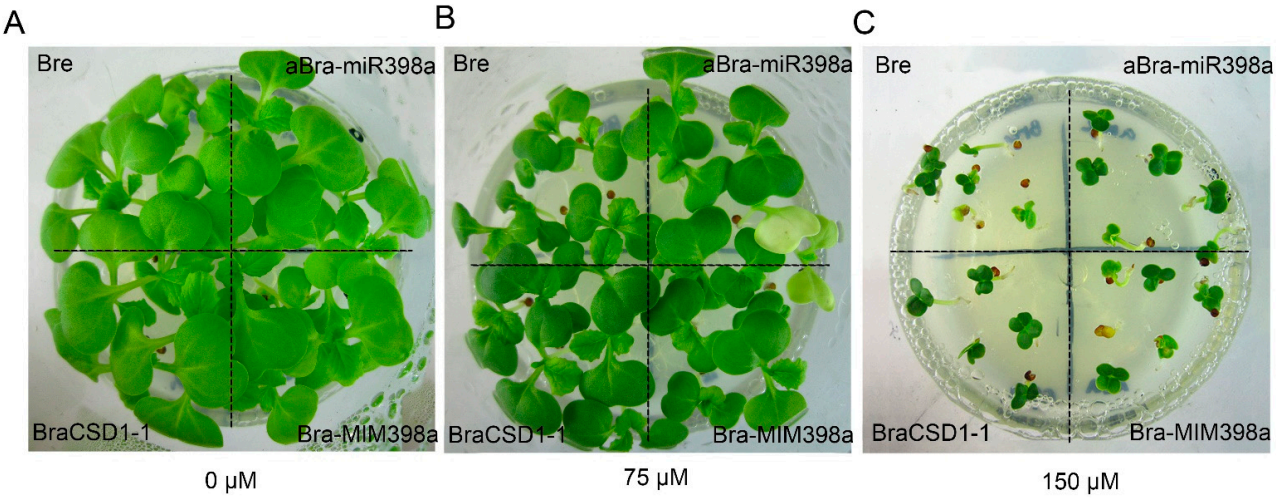

Figure 5. The phenotype of transgenic plants treated with Cu^{2+}. The seedlings of the transgenic plants growing on MS medium containing 0 μM (**A**), 75 μM (**B**), and 150 μM (**C**) Cu^{2+}, respectively.

3.5. Stress-Related Marker Genes Were Upregulated by Bra-miR398a

To further explore the role of Bra-miR398a in leaf cell death, we analyzed expression levels of some stress-related marker genes by real-time PCR. *P5CS1* gene is a rate-limiting enzyme in the biosynthesis of proline and enhances osmotic stress tolerance in transgenic plants [48]. DREB2A is a dehydration-responsive element-binding protein in plants and then activates genes that are involved in detoxification, water, and ion movement and chaperone functions [49–52]. Under high temperature, *BraLEA76*, *BraCaM1*, *BraPLC*, *BraDREB2A*, and *BraP5CS* were upregulated in *p35S::aBra-miR398a* plants (1#, 2#) (Figure 6). In addition, the expression of *BraLEA76*, *BraCaM1*, and *BraPLC* were downregulated in *35S::Bra-MIM398a* (3#, 5#) (Figure 6). These results indicated that Bra-miR398a mediated heat-induced leaf cell death possibly through these stress-related genes.

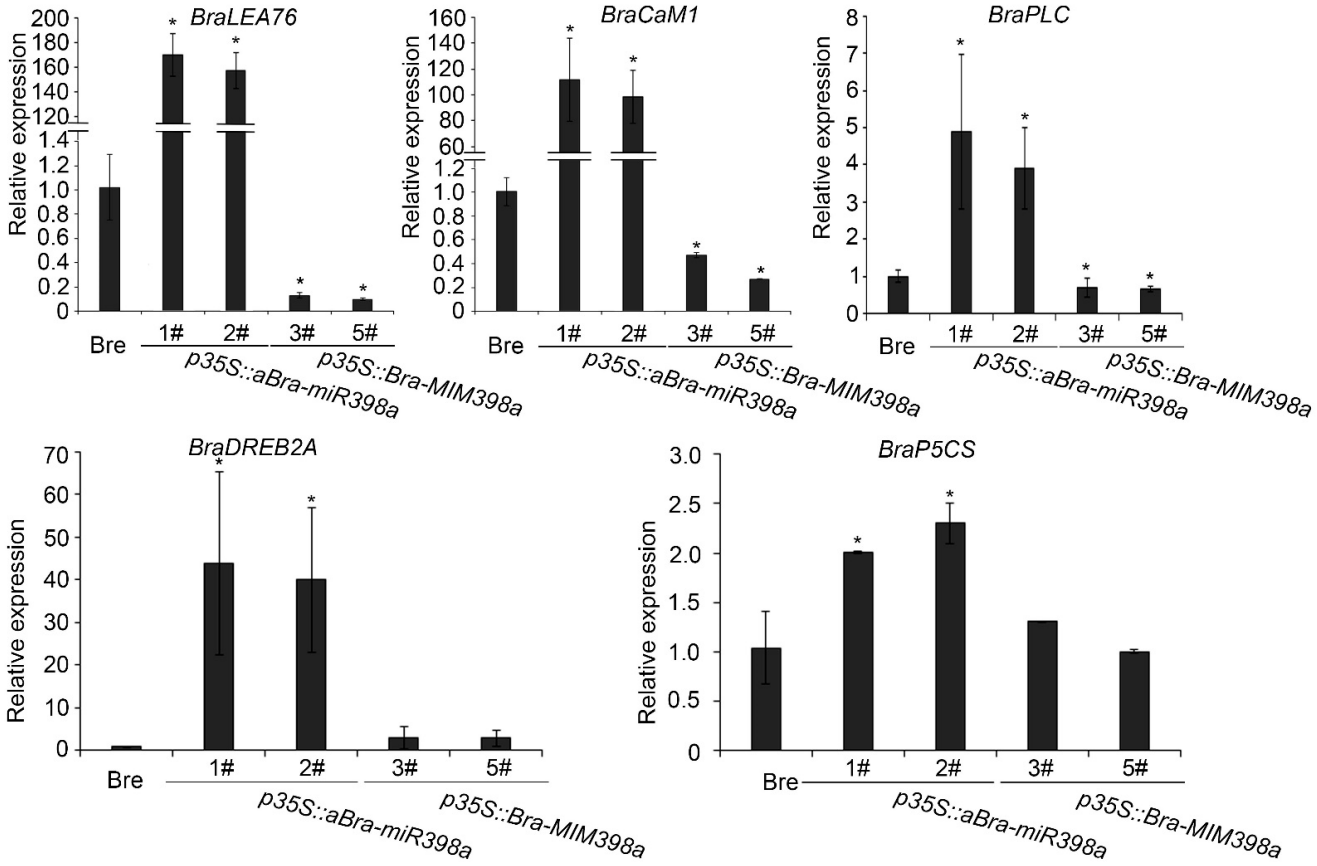

Figure 6. Expression level of cell death-related genes affected by miR398 and its targeted genes. Expression of *BraLEA76*, *BraCaM1*, *BraPLC*, *BraDREB2A*, and *BraP5CS* in Bre, *p35S::aBra-miR398a* (1#, 2#) and *p35S::Bra-MIM398a* (3#, 5#) plants at 38 °C for 1 h, respectively. The asterisks indicate a significant difference (* represents $p < 0.05$) (Student's *t*-test).

4. Discussion

miR398 is one of the miRNAs known to be involved in stress responses of the plant [53]. Enhancing of miR398 processing results in stronger plant thermotolerance [13]. In another study, the level of miR398 increased in the early senescence stage in *Arabidopsis thaliana* leaves [54]. It implies that leaf senescence and leaf cell death are related to plant thermotolerance. In this study, we provided evidence that Bra-miR398a attenuated heat-induced leaf cell death by silencing of *BraCSD1-1* gene in *B. rapa*. *B. rapa* ssp. *chinensis* and *B. rapa* ssp. *pekinensis* are two different sub-species of Brassica and the cold-resistant variety of *B. rapa* ssp. *chinensis* (Wut) is more sensitive to high temperatures as compared to *B. rapa* ssp. *pekinensis* (Bre) [46]. We found the heat response of miR398 in these two cultivars was different. The genetic variation in the *MIR398* promoter or its trans-regulatory transcription factors may contribute to the difference in the expression level of miR398 in these two sub-species. For heat stress of the whole plant, we chose 45 °C for 12 h followed by 35 °C for 12 h, which is to simulate continuous high temperature, given temperature is decreased at night. With global warming and less arable land [55], and for some high-latitude regions, it is of great significance to explore the tolerance of crops to extremely high temperatures.

Originally, we found that genetic manipulation of Bra-miR398a levels may modify the process of heat-induced leaf cell death in *B. rapa*. This conclusion is supported by the phenotype and statistical data of Bre, *p35S::Bra-MIM398a*, *p35S::BraCSD1-1*, and *p35S::aBra-miR398a* plants, as well as the expression of stress-related marker genes under heat stress. A premature senescence and leaf cell death phenotype was observed in *p35S::Bra-MIM398a* and *p35S::BraCSD1-1* plants while the senescence and leaf cell death was postponed in *p35S::aBra-miR398a* plants. Importantly, *p35S::aBra-miR398a* plants were concurrent with

higher survival rates under heat stress while the plants' high expression levels of *BraCSD1-1* (*p35S::BraCSD1-1*) concomitant with lower survival rates. Our results suggested that *BraCSD1-1* in plants might be a transcription factor and might have functions beyond a simple superoxide dismutase. In addition, the plants of Bra-miR398a overexpression up-regulates the expression of stress-related genes, *BraLEA76*, *BraCaM1*, *BraPLC*, *BraDREB2A*, and *BraP5CS* under high temperature. Together, these results showed that *BraCSD1-1* positively regulates senescence onset and progression under heat stress, while Bra-miR398a postpones these characteristics.

Several growth and development related genes also affect senescence to convey the developmental timing and implement the right timing of senescence. Although these genes might not be considered as specific regulators of senescence, it is very useful to understand the mechanism and downstream genes that implement these decisions, which contribute to the engineering plant senescence for diverse applications. Our findings indicated that Bra-miR398a is a strong candidate to control programmed cell death by inducing senescence. We believe that Bra-miR398a acts as a sensor for the unfavorable environmental condition to prevent senescence to keep the progeny safe by sensing the developmental age of the plant and transferring that information to this module further to help miR398/*CSD1* ensure the right timing of senescence and cell death. Senescence has a crucial impact on the final crop of agricultural products, in the sense that a longer growth period directly enhances the final yield by prolonging photosynthesis, so by detecting the genes which are important in this pathway, we can improve the final yield in many important crops.

Supplementary Materials: The following supporting information can be downloaded at: https://www.mdpi.com/article/10.3390/horticulturae8040299/s1, Figure S1: Overview of vector construction for amiR398 and MIM398.; Figure S2: The distribution of 5′P end reads around the miR398 target sites at BraCSD1-1 revealed by Degradome analysis; Table S1: Primer pairs used in this study; Table S2: The sequence conservation among Bra-MIR398a, Bra-MIR398b and Bra-CSDs to its *Arabidopsis thaliana* homologs at amino acid level.

Author Contributions: B.C., J.J., X.W., Y.L. and W.S. performed experiments and drafted the manuscript, J.B. performed the genetic transformation; X.Y., S.H. and Y.H. designed the research and wrote the manuscript. All authors have read and agreed to the published version of the manuscript.

Funding: This work was supported by National Programs for Science and Technology Development of China (Grant No. 2016YFD0101900) and CAS-TWAS (Chinese Academy of Sciences-The World Academy of Sciences) fellowship.

Institutional Review Board Statement: Not applicable.

Informed Consent Statement: Not applicable.

Data Availability Statement: Not applicable.

Conflicts of Interest: The authors declare no conflict of interest.

References

1. Cui, Y.; Peng, Y.; Zhang, Q.; Xia, S.; Ruan, B.; Xu, Q.; Yu, X.; Zhou, T.; Liu, H.; Zeng, D.; et al. Disruption of *EARLY LESION LEAF 1*, encoding a cytochrome P450 monooxygenase, induces ROS accumulation and cell death in rice. *Plant J.* **2021**, *105*, 942–956. [CrossRef] [PubMed]
2. Ramiro, D.A.; Melotto-Passarin, D.M.; Barbosa, M.; Santos, F.D.; Gomez, S.; Júnior, N.M.; Lam, E.; Carrer, H. Expression of *Arabidopsis Bax Inhibitor-1* in transgenic sugarcane confers drought tolerance. *Plant Biotechnol. J.* **2016**, *14*, 1826–1837. [CrossRef] [PubMed]
3. Lincoln, J.E.; Sanchez, J.P.; Zumstein, K.; Gilchrist, D.G. Plant and animal PR1 family members inhibit programmed cell death and suppress bacterial pathogens in plant tissues. *Mol. Plant Pathol.* **2018**, *19*, 2111–2123. [CrossRef] [PubMed]
4. Fraser, M.S.; Dauphinee, A.N.; Gunawardena, A.H.L.A.N. Determining the effect of calcium on cell death rate and perforation formation during leaf development in the novel model system, the lace plant (*Aponogeton madagascariensis*). *J. Microsc.* **2020**, *278*, 132–144. [CrossRef] [PubMed]
5. Woo, H.R.; Kim, H.J.; Lim, P.O.; Nam, H.G. Leaf Senescence: Systems and Dynamics Aspects. *Annu. Rev. Plant Biol.* **2019**, *70*, 347–376. [CrossRef] [PubMed]

6. Hensel, L.L.; Grbic, V.; Baumgarten, D.A.; Bleecker, A.B. Developmental and Age-Related Processes That Influence the Longevity and Senescence of Photosynthetic Tissues in Arabidopsis. *Plant Cell* **1993**, *5*, 553–564. [CrossRef] [PubMed]
7. Kim, J.; Kim, J.H.; Lyu, J.I.; Woo, H.R.; Lim, P.O. New insights into the regulation of leaf senescence in Arabidopsis. *J. Exp. Bot.* **2018**, *69*, 787–799. [CrossRef]
8. Bartel, D.P. MicroRNAs: Genomics, biogenesis, mechanism, and function. *Cell* **2004**, *116*, 281–297. [CrossRef]
9. Zhu, C.; Ding, Y.; Liu, H. MiR398 and plant stress responses. *Physiol. Plant* **2011**, *143*, 1–9. [CrossRef] [PubMed]
10. Song, X.W.; Li, Y.; Cao, X.F.; Qi, Y.J. MicroRNAs and their regulatory roles in plant-environment interactions. *Annu. Rev. Plant Biol.* **2019**, *70*, 489–525. [CrossRef] [PubMed]
11. Jones-Rhoades, M.W.; Bartel, D.P. Computational identification of plant microRNAs and their targets, including a stress-induced miRNA. *Mol. Cell* **2004**, *14*, 787–799. [CrossRef] [PubMed]
12. Sunkar, R.; Zhu, J.K. Novel and stress-regulated microRNAs and other small RNAs from Arabidopsis. *Plant Cell* **2004**, *16*, 2001–2019. [CrossRef]
13. Li, Y.; Li, X.; Yang, J.; He, Y. Natural antisense transcripts of *MIR398* genes suppress microR398 processing and attenuate plant thermotolerance. *Nat. Commun.* **2020**, *11*, 5351. [CrossRef] [PubMed]
14. Bouché, N. New insights into miR398 functions in Arabidopsis. *Plant Signal. Behav.* **2010**, *6*, 684–686. [CrossRef] [PubMed]
15. Bonnet, E.; Wuyts, J.; Rouze, P.; Van, D.P.Y. Detection of 91 potential conserved plant microRNAs in *Arabidopsis thaliana* and *Oryza sativa* identifies important target genes. *Proc. Natl. Acad. Sci. USA* **2004**, *101*, 11511–11516. [CrossRef] [PubMed]
16. Guan, Q.; Lu, X.; Zeng, H.; Zhang, Y.; Zhu, J. Heat stress induction of *miR398* triggers a regulatory loop that is critical for thermotolerance in Arabidopsis. *Plant J.* **2013**, *74*, 840–851. [CrossRef]
17. Jagadeeswaran, G.; Saini, A.; Sunkar, R. Biotic and abiotic stress down-regulate miR398 expression in *Arabidopsis*. *Planta* **2009**, *229*, 1009–1014. [CrossRef] [PubMed]
18. Sunkar, R.; Kapoor, A.; Zhu, J.K. Posttranscriptional induction of two Cu/Zn superoxide dismutase genes in *Arabidopsis* is mediated by downregulation of miR398 and important for oxidative stress tolerance. *Plant Cell* **2006**, *18*, 2051–2065. [CrossRef]
19. Abdel-Ghany, S.E.; Pilon, M. MicroRNA-mediated systemic down-regulation of copper protein expression in response to low copper availability in *Arabidopsis*. *J. Biol. Chem.* **2008**, *283*, 15932–15945. [CrossRef]
20. Jia, X.; Wang, W.X.; Ren, L.; Chen, Q.J.; Mendu, V.; Willcut, B.; Dinkins, R.; Tang, X.; Tang, G. Differential and dynamic regulation of miR398 in response to ABA and salt stress in *Populus tremula* and *Arabidopsis thaliana*. *Plant Mol. Biol.* **2009**, *71*, 51–59. [CrossRef] [PubMed]
21. Yamasaki, H.; Abdel-Ghany, S.E.; Cohu, C.M.; Kobayashi, Y.; Shikanai, T.; Pilon, M. Regulation of copper homeostasis by micro-RNA in *Arabidopsis*. *J. Biol. Chem.* **2007**, *282*, 16369–16378. [CrossRef]
22. Larkindale, J.; Mishkind, M.; Vierling, E. *Plant Abiotic Stress*; Jenks, M.A., Hasegawa, P.M., Eds.; Blackwell: Burlington, NC, USA, 2005; pp. 100–144.
23. Tian, X.; Wang, F.; Zhao, Y.; Lan, T.; Yu, K.; Zhang, L.; Qin, Z.; Hu, Z.; Yao, Y.; Ni, Z.; et al. Heat shock transcription factor A1b regulates heat tolerance in wheat and Arabidopsis through OPR3 and jasmonate signalling pathway. *Plant Biotechnol. J.* **2020**, *18*, 1109–1111. [CrossRef] [PubMed]
24. Battisti, D.S.; Naylor, R.L. Historical warnings of future food insecurity with unprecedented seasonal heat. *Science* **2009**, *323*, 240–244. [CrossRef] [PubMed]
25. Sunkar, R.; Li, Y.F.; Jagadeeswaran, G. Functions of microRNAs in plant stress responses. *Trends Plant Sci.* **2012**, *17*, 196–203. [CrossRef] [PubMed]
26. Zhai, Z.H.; Lin, Z.G.; Chen, H.H.; Chen, Z.H.; Center, G.C. Temporal and spatial variation of temperature suitability index for Brassica parachinesis in Guangdong. *Guangdong Agric. Sci.* **2016**, *3*, 66–71.
27. Jiang, J.; Bai, J.; Li, S.; Li, X.; Yang, L.; He, Y. HTT2 promotes plant thermotolerance in *Brassica rapa*. *BMC Plant Biol.* **2018**, *18*, 127. [CrossRef] [PubMed]
28. Li, X.; Zhang, S.; Bai, J.; He, Y. Tuning growth cycles of Brassica crops via natural antisense transcripts of BrFLC. *Plant Biotechnol. J.* **2016**, *14*, 905–914. [CrossRef] [PubMed]
29. Ren, W.; Wu, F.; Bai, J.; Li, X.; Yang, X.; Xue, W.; Liu, H.; He, Y. BcpLH organizes a specific subset of microRNAs to form a leafy head in Chinese cabbage (*Brassica rapa* ssp. *pekinensis*). *Hortic. Res.* **2020**, *7*, 1. [CrossRef]
30. Schwab, R.; Ossowski, S.; Riester, M.; Warthmann, N.; Weigel, D. Highly specific gene silencing by artificial microRNAs in *Arabidopsis*. *Plant Cell* **2006**, *18*, 1121–1133. [CrossRef]
31. Schwab, R.; Palatnik, J.F.; Riester, M.; Schommer, C.; Schmid, M.; Weigel, D. Specific effects of microRNAs on the plant transcriptome. *Dev. Cell* **2005**, *8*, 517–527. [CrossRef]
32. Franco-Zorrilla, J.M.; Valli, A.; Todesco, M.; Mateos, I.; Puga, M.I.; Rubio-Somoza, I.; Leyva, A.; Weigel, D.; Garcia, J.A.; Paz-Ares, J. Target mimicry provides a new mechanism for regulation of microRNA activity. *Nat. Genet* **2007**, *39*, 1033–1037. [CrossRef] [PubMed]
33. Nooden, L.D.; Hillsberg, J.W.; Schneider, M.J. Induction of leaf senescence in *Arabidopsis thaliana* by long days through a light-dosage effect. *Physiol. Plant.* **1996**, *96*, 491–495. [CrossRef]
34. He, Y.; Bai, J.; Wu, F.; Mao, Y. *In planta* transformation of *Brassica rapa* and *B. napus* via vernalization-infiltration methods. *Protoc. Exch.* **2013**. [CrossRef]

35. Liu, Z.; Jia, L.; Wang, H.; He, Y. HYL1 regulates the balance between adaxial and abaxial identity for leaf flattening via miRNA-mediated pathways. *J. Exp. Bot.* **2011**, *62*, 4367–4381. [CrossRef] [PubMed]
36. Chen, C.; Ridzon, D.A.; Broomer, A.J.; Zhou, Z.; Lee, D.H.; Nguyen, J.T.; Barbisin, M.; Xu, N.L.; Mahuvakar, V.R.; Andersen, M.R.; et al. Real-time quantification of microRNAs by stem-loop RT-PCR. *Nucleic Acids Res.* **2005**, *33*, e179. [CrossRef] [PubMed]
37. Varkonyi-Gasic, E.; Wu, R.; Wood, M.; Walton, E.F.; Hellens, R.P. Protocol: A highly sensitive RT-PCR method for detection and quantification of microRNAs. *Plant Methods* **2007**, *3*, 12. [CrossRef]
38. Livak, K.J.; Schmittgen, T.D. Analysis of relative gene expression data using real-time quantitative PCR and the $2^{-\Delta\Delta CT}$ Method. *Methods* **2001**, *25*, 402–408. [CrossRef] [PubMed]
39. Piast, M.; Kustrzeba-Wojcicka, I.; Matusiewicz, M.; Banas, T. Molecular evolution of enolase. *Acta Biochim. Pol.* **2005**, *52*, 507–513. [CrossRef] [PubMed]
40. Li, S.; Chen, L.; Zhang, L.; Li, X.; Liu, Y.; Wu, Z.; Dong, F.; Wan, L.; Liu, K.; Hong, D.; et al. BnaC9.SMG7b Functions as a Positive Regulator of the Number of Seeds per Silique in *Brassica napus* by Regulating the Formation of Functional Female Gametophytes. *Plant Physiol.* **2015**, *169*, 2744–2760. [CrossRef] [PubMed]
41. Wei, X.; Zhang, X.; Yao, Q.; Yuan, Y.; Li, X.; Wei, F.; Zhao, Y.; Zhang, Q.; Wang, Z.; Jiang, W.; et al. The miRNAs and their regulatory networks responsible for pollen abortion in Ogura-CMS Chinese cabbage revealed by high-throughput sequencing of miRNAs, degradomes, and transcriptomes. *Front. Plant Sci.* **2015**, *6*, 894. [CrossRef]
42. Yu, X.; Willmann, M.R.; Anderson, S.J.; Gregory, B.D. Genome-Wide Mapping of Uncapped and Cleaved Transcripts Reveals a Role for the Nuclear mRNA Cap-Binding Complex in Cotranslational RNA Decay in Arabidopsis. *Plant Cell* **2016**, *28*, 2385–2397. [CrossRef] [PubMed]
43. Martin, M. Cutadapt removes adapter sequences from high-throughput sequencing reads. *EMBnet. J.* **2011**, *17*, 10. [CrossRef]
44. Dobin, A.; Davis, C.A.; Schlesinger, F.; Drenkow, J.; Zaleski, C.; Jha, S.; Batut, P.; Chaisson, M.; Gingeras, T.R. STAR: Ultrafast universal RNA-seq aligner. *Bioinformatics* **2013**, *29*, 15–21. [CrossRef]
45. Lu, X.; Guan, Q.; Zhu, J. Downregulation of *CSD2* by a heat-inducible *miR398* is required for thermotolerance in *Arabidopsis*. *Plant Signal Behav.* **2013**, *8*, e54952. [CrossRef] [PubMed]
46. Yu, X.; Wang, H.; Lu, Y.; de Ruiter, M.; Cariaso, M.; Prins, M.; van Tunen, A.; He, Y. Identification of conserved and novel microRNAs that are responsive to heat stress in *Brassica rapa*. *J. Exp. Bot.* **2012**, *63*, 1025–1038. [CrossRef]
47. He, Y.H.; Tang, W.N.; Swain, J.D.; Green, A.L.; Jack, T.P.; Gan, S.S. Networking senescence-regulating pathways by using Arabidopsis enhancer trap lines. *Plant Physiol.* **2001**, *126*, 707–716. [CrossRef]
48. Kishor, P.; Hong, Z.; Miao, G.H.; Hu, C.; Verma, D. Overexpression of [delta]-Pyrroline-5-Carboxylate Synthetase Increases Proline Production and Confers Osmotolerance in Transgenic Plants. *Plant Physiol.* **1995**, *108*, 1387–1394. [CrossRef] [PubMed]
49. Shinozaki, K.; Yamaguchi-Shinozaki, K. Gene networks involved in drought stress response and tolerance. *J. Exp. Bot.* **2007**, *58*, 221–227. [CrossRef]
50. Wang, W.; Vinocur, B.; Altman, A. Plant responses to drought, salinity and extreme temperatures: Towards genetic engineering for stress tolerance. *Planta* **2003**, *218*, 1–14. [CrossRef]
51. Xiong, L.; Zhu, J.K. Molecular and genetic aspects of plant responses to osmotic stress. *Plant Cell Env.* **2002**, *25*, 131–139. [CrossRef]
52. Yoshida, T.; Mogami, J.; Yamaguchi-Shinozaki, K. ABA-dependent and ABA-independent signaling in response to osmotic stress in plants. *Curr. Opin. Plant Biol.* **2014**, *21*, 133–139. [CrossRef]
53. Ding, Y.F.; Wang, G.Y.; Fu, Y.P.; Zhu, C. The role of miR398 in plant stress responses. *Yi Chuan* **2010**, *32*, 129–134. [CrossRef] [PubMed]
54. Huo, X.; Wang, C.; Teng, Y.; Liu, X. Identification of miRNAs associated with dark-induced senescence in *Arabidopsis*. *BMC Plant Biol.* **2015**, *15*, 266. [CrossRef]
55. Zhu, T.; De Lima, C.F.F.; De Smet, I. The Heat is On: How Crop Growth, Development and Yield Respond to High Temperature. *J. Exp. Bot.* **2021**, *72*, 7359–7373. [CrossRef]